LA-8157-PR

Progress Report

C.3

Applied Nuclear Data Research and Development

July 1—September 30, 1979

LOS ALAMOS SCIENTIFIC LABORATORY
Post Office Box 1663 Los Alamos, New Mexico 87545

The four most recent reports in this series, unclassified, are LA-7596-PR, LA-7722-PR, LA-7843-PR, and LA-8036-PR.

This report was not edited by the Technical Information staff.

This work was performed under the auspices of the US Department of Energy's Office of Military Application, Division of Reactor Research and Technology, Office of Basic Energy Sciences, and Office of Fusion Energy; and the Electrical Power Research Institute.

UNITED STATES
DEPARTMENT OF ENERGY
CONTRACT W-7405-ENG. 36

LA-8157-PR
Progress Report

UC-34c
Issued: November 1979

Applied Nuclear Data Research and Development

July 1—September 30, 1979

Compiled by

C. I. Baxman and P. G. Young

CONTENTS

APPLIED NUCLEAR DATA RESEARCH AND DEVELOPMENT
QUARTERLY PROGRESS REPORT
July 1 - September 30, 1979

Compiled by

C. I. Baxman and P. G. Young

ABSTRACT

This progress report describes the activities of the Los Alamos Nuclear Data Group for the period July 1 through September 30, 1979. The topical content is summarized in the contents.

I. THEORY AND EVALUATION OF NUCLEAR CROSS SECTIONS

A. R-Matrix Analysis of Light Systems (G. M. Hale and D. C. Dodder)

Work has continued primarily on reactions in the 4- and 5-nucleon systems during the past quarter. These systems contain reactions of interest as fusion energy producers, as neutron sources, and as neutron standards. In addition, the 4-nucleon system in particular offers an ideal testing ground for our charge-independent R-matrix modeling.[1,2] Some significant developments along these lines are described below.

• 1. 4-Nucleons: (a) Prediction of n-T Total Cross Sections from p-^{3}He Parameters. The charge-independence of nuclear forces would imply that n-T and p-^{3}He scattering are the same process except for Coulomb differences. These Coulomb differences outside the range of nuclear forces are automatically contained in the external shift, penetrability, and hard-sphere phase functions of R-matrix theory. Coulomb differences inside the interaction region, although dominated by the nuclear forces, are usually important to take into account as perturbation effects. We have done this in the case of p-^{3}He and n-T by simply shifting the eigenvalues (E_λ) of the p-^{3}He R-matrix downward by 0.88 MeV, which is the energy difference one gets from a uniformly charged sphere calculation, to obtain the n-T R-matrix parameters. We then predict the n-T total cross section shown in

Fig. 1. Also shown in this figure are new n-T total cross-section measurements from Livermore,[3] which appear to be in good agreement with the predictions. The rise in the low-energy cross section, evident in both the measurement and the calculations as one approaches zero energy, is significant since previous measurements did not indicate its existence and since it leads to a zero-energy cross section 30% higher than the usually accepted (ENDF) value. A higher zero-energy cross section may help to resolve the discrepancy between the coherent scattering length and elastic cross section for n-T scattering.[4,5]

(b) Difference in the d-d reactions. We have been forced to conclude that isospin mixing in the external Coulomb field is not sufficient to explain the large differences observed in measurements, particularly of the cross sections in the few-hundred keV range, for the two branches of the d + d reaction. Following the suggestion of Sergeyev[6] that additional isospin mixing from the internal Cou-

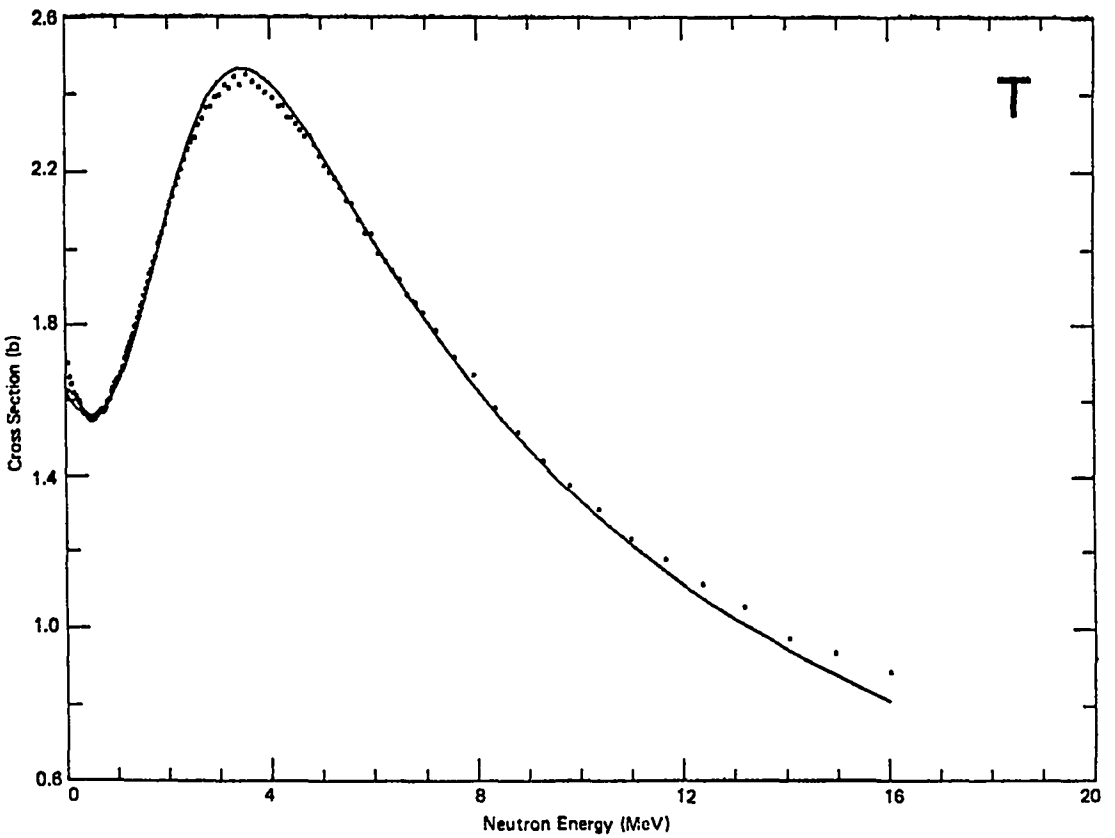

Fig. 1.
New measurements[3] of the n-T total cross section compared with R-matrix predictions (solid curve) from an analysis of p-^{3}He data.

lomb interactions may reproduce the observed differences, we have allowed non-zero isospin-1 widths in the ^3P states of the d + d channel. Indeed, the experimental differences are largely reproduced (see Fig. 2) with mixing widths only 2% of the single-particle width which characterizes the d + d widths in the ^3P isospin-0 levels. This is entirely consistent with the magnitude of the matrix element one would expect from internal Coulomb mixing, indicating that no violation of the charge independence of nuclear forces is required to explain even the large differences between measurements for the D(d,p) and D(d,n) reactions. We are continuing to study this problem using polarization data measured at ETH (Zurich) and at Ohio State specifically to probe differences in the d + d reactions.

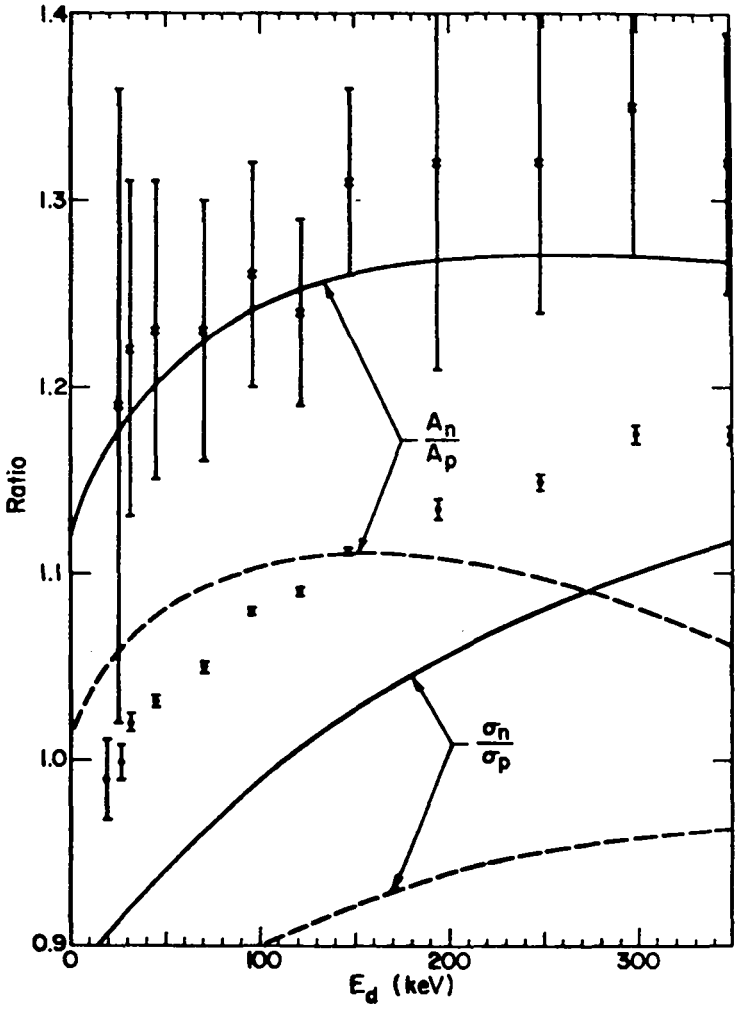

Fig. 2.
Ratios of the integrated cross sections and of the asymmetries, $A = \frac{\sigma(0)}{\sigma(90)}$, for the two branches of the d + d reaction. The points are measurements of Theus et al.; the solid and dashed curves are R-matrix calculations with and without internal isospin mixing, respectively.

2. 5 Nucleons: ^{5}He Analysis. New preliminary data from Ohio State for the T(d,n)^{4}He reaction measured with polarized deuterons at energies between 3 and 6 MeV indicate that some of the data included in our analysis of reactions in the ^{5}He system may be incorrect. The new data have been included in our analysis, and appear to be accommodated with small adjustments in the R-matrix parameters that do not affect the low energy T(d,n) cross sections very much. However, large discrepancies remain between the fit and some of the previous measurements for the reaction at 7 MeV.

B. Evaluation of Iron Cross Sections up to 40 MeV (E. D. Arthur and P. G. Young)

To provide data for the Fusion Materials Irradiation Test Facility (FMIT), we have evaluated neutron cross sections on iron up to 40 MeV. Our results were joined to the ENDF/B-V evaluation around 3 MeV. Since little neutron experimental data exist above 20 MeV, we relied on nuclear model calculations to provide a majority of the evaluated cross sections and emission spectra. Our calculations on ^{54,56}Fe were performed only after extensive efforts were made to determine input parameters--optical model sets, gamma-ray strength functions, nuclear level densities, etc.--applicable over the entire energy range of interest. For neutron optical parameters we followed the method of Lagrange[7] in which total, elastic, and nonelastic data were supplemented by resonance information to determine the parameters shown in Table I. For protons and alpha particles we used published[8,9] optical sets obtained in the mass and energy region of interest to the present calculations. These were then modified to better reproduce data at low and high incident energies by comparison to (p,n), (α,n), and σ_R values.

Following the method of Gardner,[10] we used gamma-ray strength functions to describe gamma-ray emission that prevented problems arising from the normalization of gamma-ray transmission coefficients to s-wave average resonance values $\langle\Gamma_\gamma\rangle$ and $\langle D\rangle$. Nuclei throughout the calculation were described using a combination of the maximum available discrete level information along with the Gilbert-Cameron level density[11] with Cook parameters[12] at higher excitation energies. Preequilibrium effects, important in this incident energy region, were included through use of the Kalbach master equation model.[13]

Two general types of calculations were performed. Since direct reaction effects are present resulting from inelastic scattering from ^{54,56}Fe collective

TABLE I

NEUTRON OPTICAL PARAMETERS FOR IRON

	r(fm)	a(fm)
$V(MeV) = 49.747-0.4295E-0.0003E^2$	1.2865	0.561
$W_{SD}(MeV) = 6.053+0.074E$	1.3448	0.473
Above 6 MeV		
$W_{SD}(MeV) = 6.497-0.325(E-6.)$		
$W_{vol}(MeV) = -0.207+0.253E$	1.3448	0.473
$V_{SO}(MeV) = 6.2$	1.12	0.47

states, we made DWBA calculations using the optical parameters of Table I and deformation parameters determined from proton inelastic scattering.[14] These direct cross sections were used to renormalize the reaction cross section available for multistep particle emission calculated using the GNASH preequilibrium statistical model code.[15]

Figure 3 illustrates major cross sections calculated for ^{56}Fe from 10-40 MeV. Since some processes involve complex chains (for example, n,2np = n,2np + n,npn + n,p2n) and since gamma-ray production information was needed, it was necessary to include as many as 20 reaction types at higher energies. To check our parameters for the higher energy region, we performed $^{56}Fe(p,xn)$ calculations up to 40 MeV that are compared to experimental data[16,17] in Fig. 4.

Several neutron data types provide constraints on our calculations. Figure 5 compares our calculated neutron emission spectra to experimental data[18,19] at 14.6 MeV. By agreeing with these data at lower energies, more confidence can be placed in our calculations at higher energies where no data exist. The predicted neutron spectrum at 36 MeV appears in Fig. 6 where discrete level cross sections calculated using DWBA methods are apparent. The breaks in the continuum region result from the representation used to introduce angular distribution effects. (At present ENDF/B-V has no straightforward way to represent energy-angle correlations in the continuum.) Since higher energy components of such emission spectra are strongly forward peaked, the resulting evaluation would be unphysical if

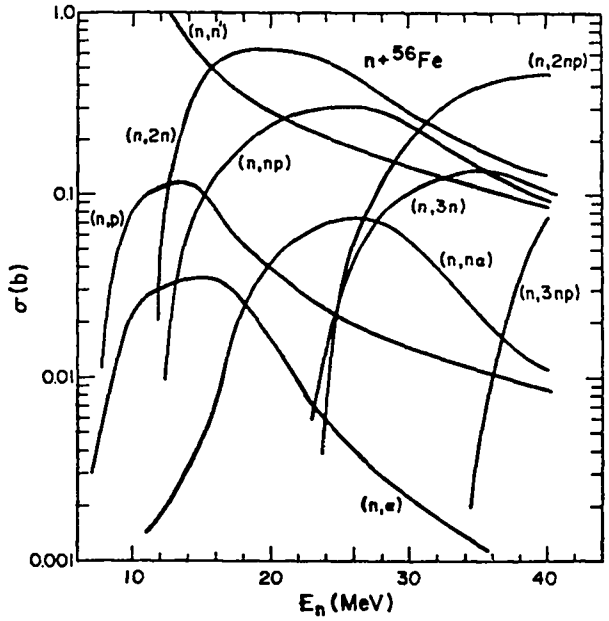

Fig. 3.
Calculated cross sections for the n + ^{56}Fe up to 40 MeV.

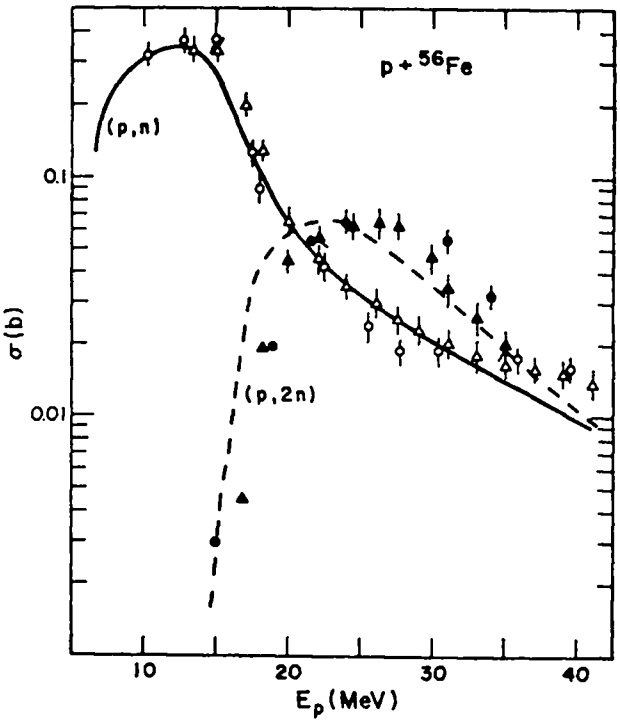

Fig. 4.
Calculated and experimental[16,17] cross sections for ^{56}Fe(p,xn) reactions.

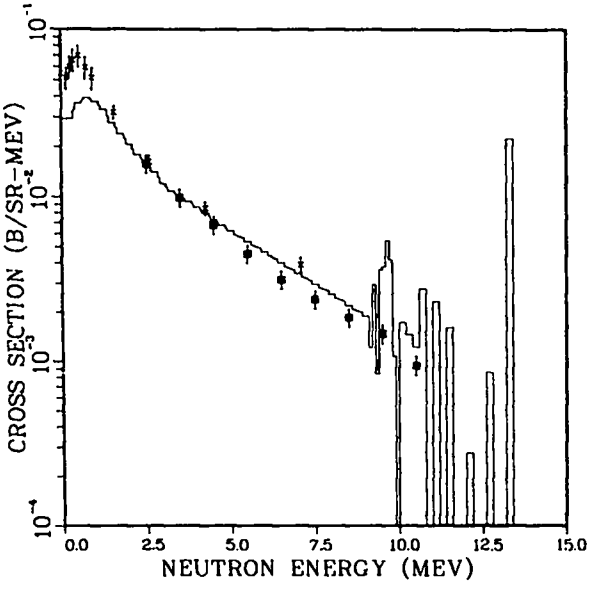

Fig. 5.
Comparison of calculated and experimental[18,19] results for neutron emission induced by 14.6-MeV neutrons.

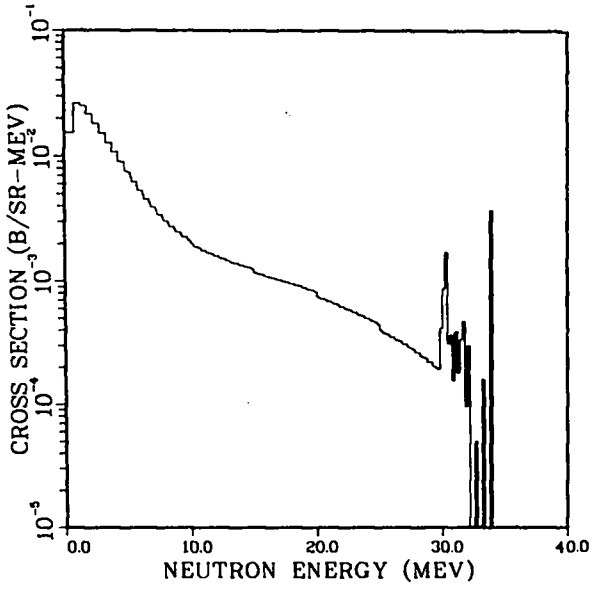

Fig. 6.
The calculated neutron emission spectrum at 90° for 36-MeV neutron incident on iron.

such effects were neglected. We therefore divided the continuum region into 5-MeV wide secondary energy bins and applied the phenomenological expressions of Kalbach[20] to determine an angular distribution for each bin. The average energy in each bin was used for this determination, which lead to the discontinuities shown at the boundaries of each bin. Further examples of the angular distribution information provided in this evaluation are shown in Fig. 7a where the DWBA angular distribution is compared to data[21,22] for inelastic scattering from the 0.846-MeV state by 14-MeV neutrons, while in Fig. 7b continuum angular distributions measured by Hermsdorf[19] are compared to the predictions of the Kalbach systematics[20] used throughout our calculations.

Gamma-ray production spectra have been measured[23] up to 20 MeV. Since our calculated spectra generally are in agreement (see Fig. 8), we have some confidence in the parameters used to produce the 40-MeV gamma-ray production spectrum shown in Fig. 9.

Among the cross-section types of interest to our evaluation are total proton and alpha-particle production cross sections. These are of some importance since such data are to be used for charged-particle damage studies at higher energies. The proton and alpha production cross sections are shown in Fig. 10 for $^{54,56}Fe$, where a comparison at 15 MeV is made to the recent measurements by Grimes et al.[24]

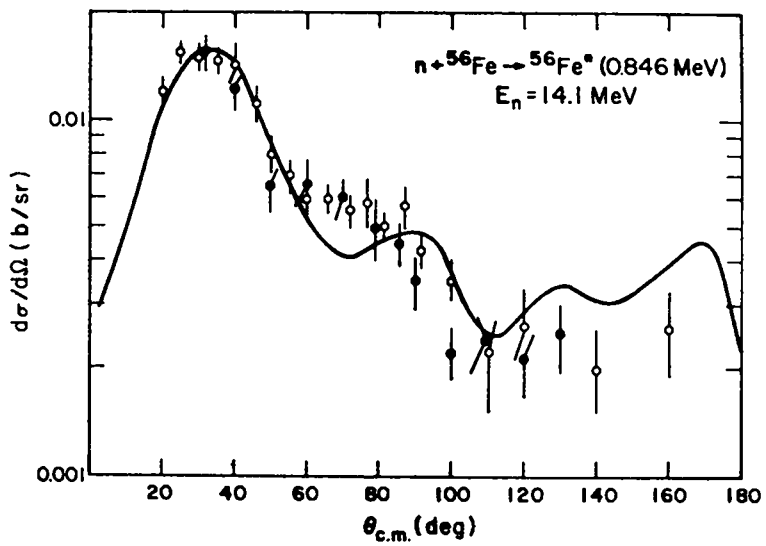

Fig. 7a.
The experimental and theoretical angular distributions are compared for excitation of the 0.846-MeV level by 14-MeV neutrons.

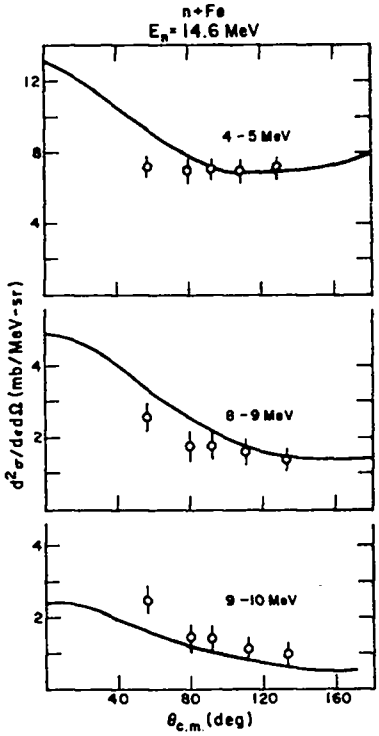

Fig. 7b.
Continuum neutron angular distributions for selected secondary energy ranges measured by Hermsdorf[19] are compared to the prediction of the Kalbach[20] systematics.

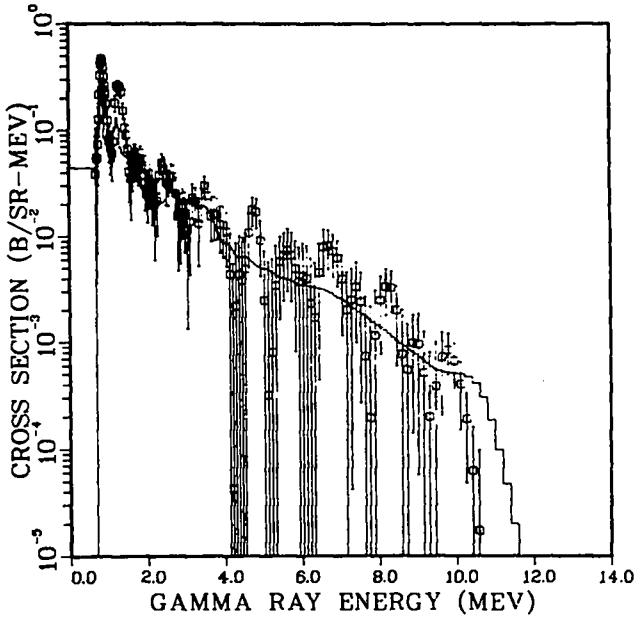

Fig. 8.
Gamma-ray production measured by Chapman et al.[23] are compared to our n + Fe results at 18 MeV.

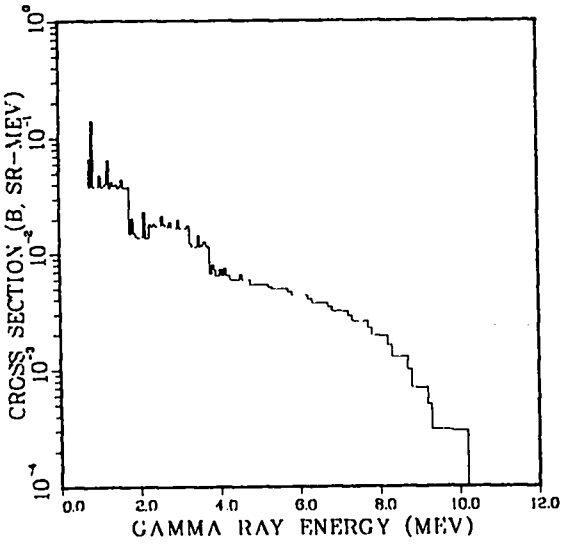

Fig. 9.
The predicted gamma-ray production spectra for 40-MeV neutrons incident on Fe.

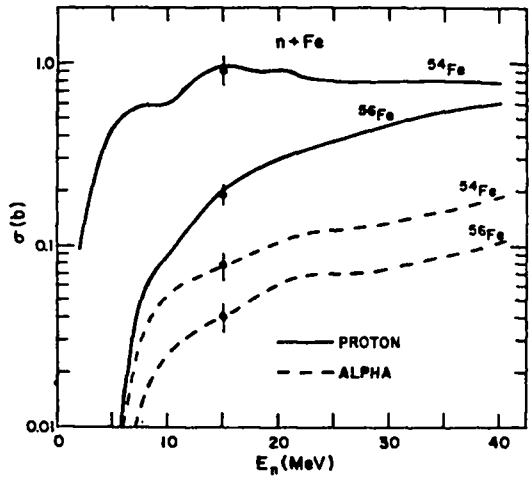

Fig. 10.
Theoretical predictions of the integrated charged-particle production cross sections up to 40 MeV are compared to the data of Grimes et al. (Ref. 24).

C. ^{241}Pu Evaluation [O. Bersillon and Ch. Lagrange (Bruyères-le-Châtel) and D. Madland

A collaborative effort between Bruyères-le-Châtel (France) and the Los Alamos Scientific Laboratory (LASL) has begun on the evaluation of neutron induced reactions on ^{241}Pu. Experimental data for this nucleus are sparse, consisting mainly of fission and capture cross-section data and low energy total cross-section data. Consequently, the evaluation will rely heavily upon theoretical model calculations. Preliminary coupled-channel optical-model calculations have been performed to determine total, elastic, and direct inelastic scattering cross sections, as well as transmission coefficients for use in Hauser-Feshbach calculations. The codes JUPITOR[25] and ECIS-78[26] were used. A preliminary test Hauser-Feshbach calculation has also been performed using the code COMNUC[27] with transmission coefficients generated from a spherical optical-model potential. The preliminary results are currently under study.

D. Calculation of Prompt Fission Neutron Spectra [D. G. Madland and J. R. Nix (T-9)]

The status of the prompt fission neutron spectrum calculations is to be summarized at the International Conference on Nuclear Cross Sections for Technology.[28] Work is continuing on calculations using energy-dependent compound-nucleus formation cross sections for comparisons with experimental prompt neutron spectrum data from several different fissioning systems. Calculations of the average number of prompt neutrons per fission, $\bar{\nu}_p$, using the formalism developed for the fission spectrum calculations are also in progress.

II. NUCLEAR CROSS SECTION PROCESSING

A. Thermal Reactor Cross Section Libraries from ENDF/B-V (R. E. MacFarlane)

The NJOY nuclear data processing system has been used to produce cross-section libraries for EPRI-CELL and EPRI-CPM. As an initial validation of these libraries, four CSEWG thermal lattice benchmarks[29] have been analyzed. In addition, the validity of the approximate methods used in CELL and CPM have been tested by comparison with Monte-Carlo results for a simple infinite cell provided by R. Prael of the LASL Monte Carlo Group X-6.

The infinite cell results are summarized in Tables II and III. Note that the methods compare very well for the oxide case (BAPL-1) except for the CPM prediction of ^{235}U resonance self-shielding. For the metal rod (TRX-1), there are more

TABLE II

BAPL-1 INFINITE CELL (ENDF/B-V)

Quantity	MCNP	CPM	CELL
k_∞	1.1417	1.1379	1.1388
ρ_{28}	1.401	1.382	1.388
δ_{25}	0.0832	0.0793	0.0818
δ_{28}	0.0715	0.0707	0.0707
C*	0.8088	0.8051	0.8093
^{235}U fiss	1.285	1.289	1.274
	1.652	1.655	1.632
	25.52	24.25	25.31
	366.8	366.0	365.24
^{235}U abs	1.350	1.345	1.339
	2.117	2.123	2.091
	38.08	36.85	38.23
	430.0	428.1	428.2
^{238} fiss	0.3916	0.3951	0.3909
	5.01-4	4.89-4	4.73-4
	1.06-4	1.03-4	1.02-4
	3.50-6	3.49-6	3.48-6
^{238}U abs	0.4491	0.4340	0.4478
	0.2631	0.2540	0.2513
	2.007	2.007	2.020
	1.8003	1.796	1.794

TABLE III

TRX-2 INFINITE CELL (ENDF/B-V)

Quantity	MCNP	CPM	CELL
k_∞	1.1679	1.1590	1.1598
ρ_{28}	0.8286	0.8423	0.8211
δ_{25}	0.05997	0.05739	0.05851
δ_{28}	0.06598	0.06507	0.06513
C*	0.6381	0.6443	0.6401
^{235}U fiss	1.433	1.441	1.413
	1.707	1.718	1.639
	24.87	23.54	24.34
	331.7	329.8	324.5
^{235}U abs	1.504	1.502	1.483
	2.178	2.195	2.079
	36.88	35.70	36.53
	388.6	386.5	380.2
^{238}U fiss	0.4407	0.4426	0.4379
	5.42-4	5.32-4	5.02-4
	7.82-5	9.20-5	8.83-5
	3.16-6	3.14-6	3.09-6
^{238}U abs	0.5124	0.4839	0.5002
	0.2670	0.2579	0.2445
	1.547	1.602	1.562
	1.625	1.616	1.590

problems. The CELL thermal cross sections are low, the CELL high-energy cross sections are low, and the CPM ^{238}U resonance absorption is high. The second problem probably results from the approximate "heterogeneous fast effect," which was designed for oxide pins. The other two effects will require further study.

The CELL and CPM benchmark results are given in Tables IV and V (see Table VI for the experimental values of the integral parameters). The CELL results are fairly good and reasonably consistent. The ^{238}U resonance capture for ENDF/B-V is still a little too large (these k_{eff} values are lower than the previous ones due to an error in the thermal transport cross sections in the preliminary library). CPM compares well with CELL except for the metal lattices due to the tendency to over-estimate ^{238}U absorption noted in connection with the Monte-Carlo results.

The problems with the metal lattices should be studied in order to improve the overall reliability and usefulness of the codes. However, the oxide results give some confidence that the ENDF/B-V libraries will be usable for practical reactor problems.

B. Critical Mass Calculations for ^{242}Pu (R. B. Kidman)

In support of T-2's ^{242}Pu cross-section evaluation effort, critical masses for bare ^{242}Pu spheres have been calculated from several different data sets using varying densities and numbers of groups. The calculations were performed with the ONEDA code using $S_n = 16$, $P_\ell = 3$, and 50 mesh intervals.

Results are presented in Table VII and compared to earlier 30-group and Monte Carlo calculations by Soran and Barrett.[30] The present ENDF/B-IV calculations were made with the LIB-IV library,[31] which is a 50-group fast reactor data set. Similarly, the ENDF/B-V calculations were made with LIB-V, which is a 70-group library that has recently been distributed.

C. Neutron and Gamma-Ray Data for Activation Calculations (M. E. Battat, R. J. LaBauve, and D. C. George)

A data library entitled "GAMMON" was completed during this quarter, and a report[32] describing this work has been published. This activation library contains multigroup cross section data in 100 groups for 420 important neutron-induced reactions and multigroup gamma-ray spectra in 25 groups for 107 unique daughter products. The file also contains maximum permissible concentrations for 200 reaction products and "absorbable" decay energy for 85 products.

TABLE IV

EPRI-CELL CSEWG BENCHMARKS (ENDF/B-V)

Quantity	BAPL-1	BAPL-3	TRX-1	TRX-2
k_∞	1.1366	1.1289	1.1749	1.1583
k_{eff}	0.9975	0.9992	0.9953	0.9938
ρ_{28}	1.424	0.9233	1.348	0.8448
δ_{25}	0.08356	0.05222	0.0977	0.0599
δ_{28}	0.07451	0.05268	0.0967	0.0688
C*	0.81659	0.6629	0.7978	0.6439
^{235}U fiss	1.274	1.322	1.320	1.412
	1.629	1.634	1.625	1.635
	25.18	25.55	23.93	24.20
	365.2	380.4	321.8	324.5
^{235}U abs	1.339	1.388	1.388	1.483
	2.086	2.085	2.072	2.073
	38.06	38.64	35.91	36.36
	428.2	445.6	377.4	380.2
^{238}U fiss	0.3895	0.4111	0.3990	0.4359
	4.76-4	4.90-4	4.81-4	5.06-4
	1.02-4	1.00-4	9.13-5	8.90-5
	3.48-6	3.60-6	3.08-6	3.10-6
^{238}U abs	0.4467	0.4692	0.4591	0.4985
	0.2502	0.2510	0.2421	0.2434
	2.018	2.136	1.503	1.561
	1.794	1.855	1.590	1.590

TABLE V

EPRI-CPM CSEWG BENCHMARKS (ENDF/B-V)

Quantity	BAPL-1	BAPL-3	TRX-1	TRX-2
k_∞	1.1379	1.1297	1.1686	1.1590
k_{eff}	0.9968	0.9991	0.9884	0.9937
ρ_{28}	1.419	0.9265	1.394	0.8676
δ_{25}	0.08124	0.05114	0.09599	0.0590
δ_{28}	0.07485	0.05272	0.09777	0.0691
C*	0.8163	0.6634	0.8147	0.6523
^{235}U fiss	1.289	1.341	1.342	1.441
	1.654	1.675	1.672	1.717
	24.17	24.69	23.12	23.47
	365.6	382.2	322.8	329.6
^{235}U abs	1.345	1.397	1.400	1.503
	2.120	2.146	2.139	2.192
	36.75	37.51	35.12	35.60
	428.6	447.7	378.6	386.1
^{238}U fiss	0.3942	0.4163	0.4030	0.4413
	4.93-4	5.09-4	5.06-4	5.37-4
	1.04-4	1.02-4	9.51-5	9.26-5
	3.48-6	3.62-6	3.09-6	3.14-6
^{238}U abs	0.4449	0.4556	0.4445	0.4833
	0.2536	0.2563	0.2520	0.2574
	2.005	2.134	1.550	1.601
	1.795	1.862	1.595	1.615

TABLE VI

CSEWG BENCHMARK EXPERIMENTAL VALUES

Quantity	BAPL-1	BAPL-3	TRX-1	TRX-2
k_{eff}	1.0	1.0	1.0	1.0
ρ_{28}	1.390 ± 0.010	0.906 ± 0.10	1.311 ± 0.020	0.830 ± 0.015
δ_{25}	0.084 ± 0.002	0.052 ± 0.001	0.0981 ± 0.0010	0.0608 ± 0.0007
δ_{28}	0.078 ± 0.004	0.057 ± 0.003	0.0914 ± 0.0020	0.0667 ± 0.0020

TABLE VII

^{242}Pu CRITICAL MASS CALCULATIONS

Cross Sections	Chi	No. of Groups	Density (g.cc)	Radius (cm)	Mass (kg)	Source
ENDF/B-IV	ENDF/B-IV	50	16.071	8.8342	46.431	Present work
ENDF/B-V (Prel)	ENDF/B-IV	50	16.071	9.9991	67.159	"
ENDF/B-V (Prel)	ENDF/B-V (Prel)	50	16.071	12.2308	123.218	"
ENDF/B-V (Prel)	ENDF/B-V (Prel)	50	19.5	10.0884	83.902	"
ENDF/B-V	ENDF/B-V	70	19.5	10.0974	84.126	"
ENDF/B-V	ENDF/B-V	70	19.86	9.9141	81.098	"
ENDF/B-V (Prel)	ENDF/B-V (Prel)	30	19.5	9.8185	77.31	Soran & Barrett
ENDF/B-V	ENDF/B-V	30	19.5	10.2098	86.93	"
ENDF/B-V (Prel)	ENDF/B-V (Prel)	*	19.5	9.65	73.40	"
ENDF/B-V	ENDF/B-V	*	19.5	10.12	84.66	"

*Continuous energy Monte Carlo calculations.

A small code entitled BIGAMON was written to retrieve the data from GAMMON and rebin it into broader multigroups. A report describing the code is being published.

The GAMMON data file, the BIGAMON code, and sample problems will be sent to the Radiation Shielding Information Center (RSIC) at Oak Ridge National Laboratory (ORNL) as soon as the reports are issued.

III. FISSION PRODUCTS AND ACTINIDES: YIELDS, DECAY DATA, DEPLETION, AND BUILDUP

A. ENDF/B-V Yields (T. R. England and N. L. Whittemore)

A report was prepared for inclusion in the 3rd ASTM EURATOM Symposium on Reactor Dosimetry held in Ispra, Italy, on October 1-5, 1979, on the status of ENDF/B-V yields.[33] Comparison plots of several yield sets are shown in Figs. 11-14.

B. ORNL ^{239}Pu Decay Spectra (T. R. England, N. L. Whittemore, and D. C. George)

For a joint report to be issued by ORNL (J. K. Dickens as lead author), the recent ORNL ^{239}Pu beta and gamma spectral measurements have been compared with CINDER-10 calculations (ENDF/B-IV decay data). This is a severe test of the calculational data base because of the short irradiation histories and cooling times of the ORNL samples (1, 5, and 100 s).

Six of the forty-eight comparisons supplied for the report are given in Figs. 15-20. These apply at the mid-range of cooling times for each of the three irradiation times.

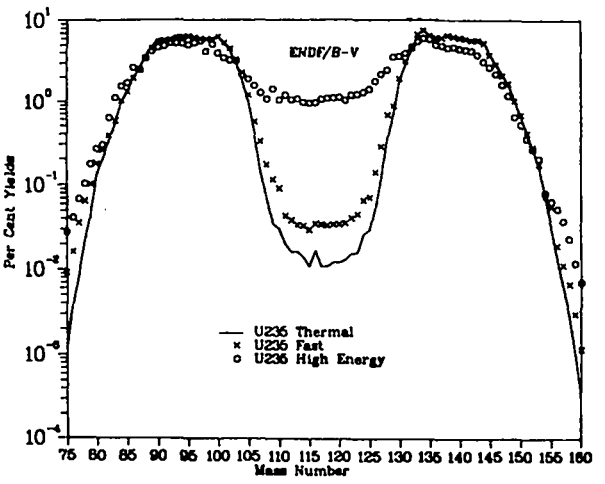

Fig. 11.
Chain yields vs. mass number.

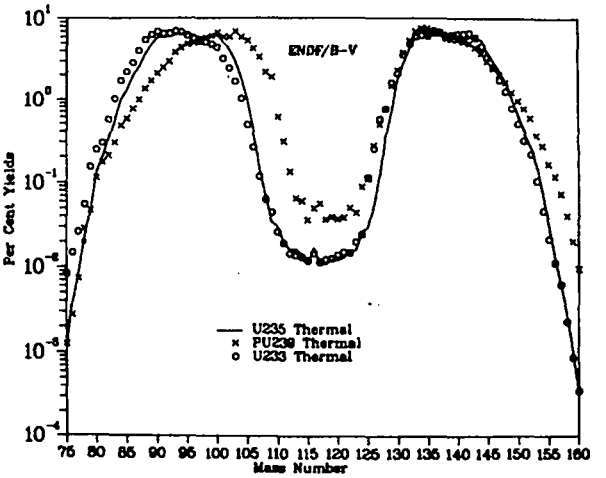

Fig. 12.
Chain yields vs. mass number.

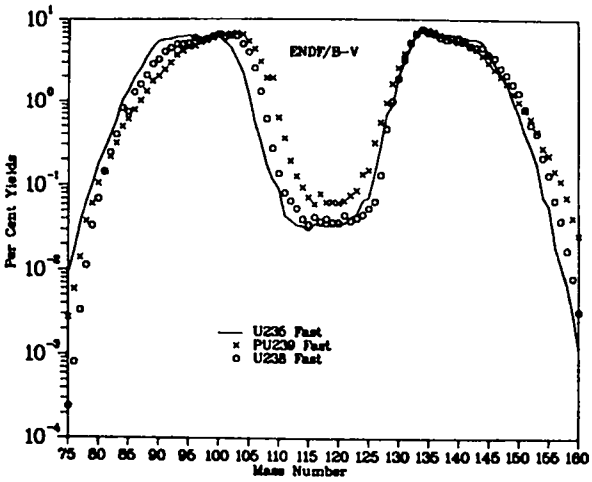

Fig. 13.
Chain yields vs. mass number.

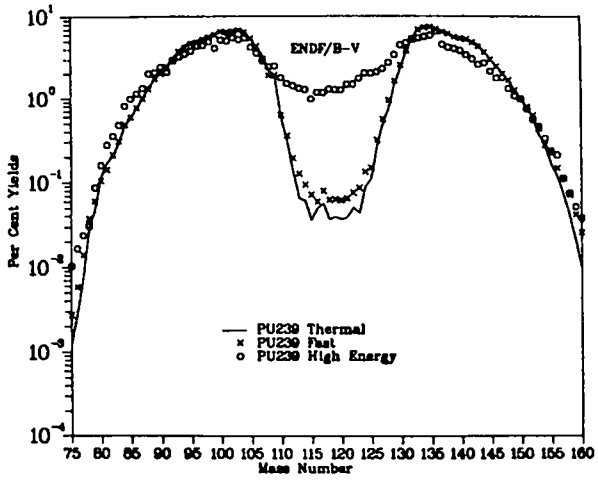

Fig. 14.
Chain yields vs. mass number

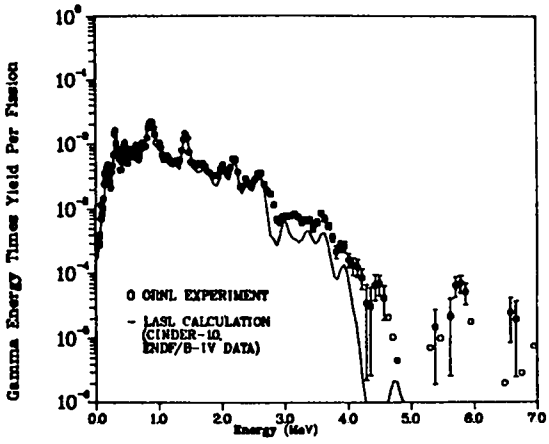

Fig. 15.
^{239}Pu thermal fission, 100 s irradiation, 2700.0 s decay.

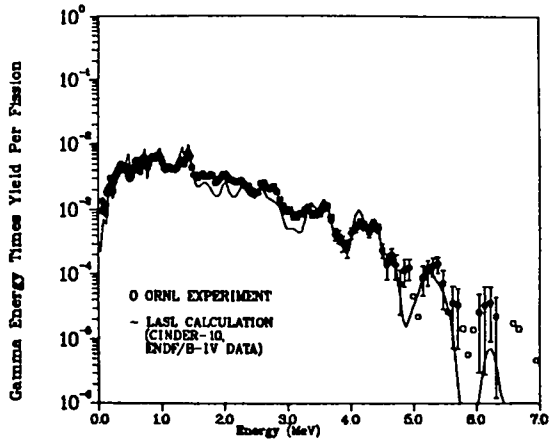

Fig. 16.
^{239}Pu thermal fission, 5 s irradiation, 197.7 s decay.

C. TMI-2 Decay Power and Radioactivity (W. B. Wilson, T. R. England, and N. L. Whittemore)

An extensive effort to provide data on decay power and related quantities for the President's Commission on the Accident at Three Mile Island was completed in August and a report was prepared.[34] The report contains detailed nuclide summary data for TMI-2, comparison data for other reactors, and a survey of heating following a wide range of irradiation times. The cooling time-dependent values of each gas and each important product for TMI-2 and comparison data for a long-lived reactor are also included in the report, along with other requested data. Subsequent to completion of this report, the Commission requested data on total

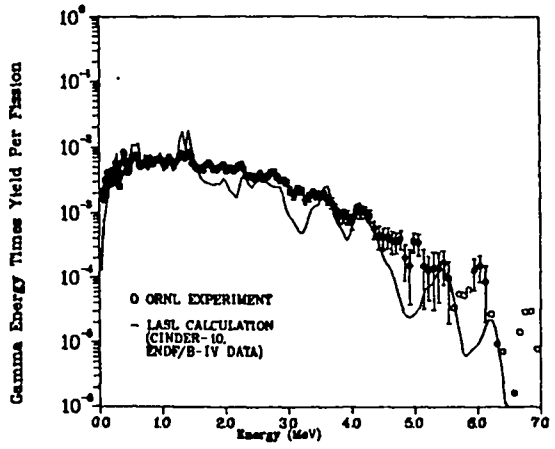

Fig. 17.
^{239}Pu thermal fission, 1 s irradiation, 29.7 decay.

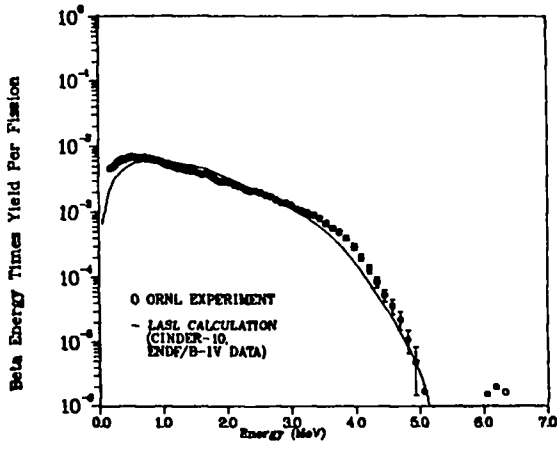

Fig. 18.
^{239}Pu thermal fission, 100 s irradiation, 2700.0 decay.

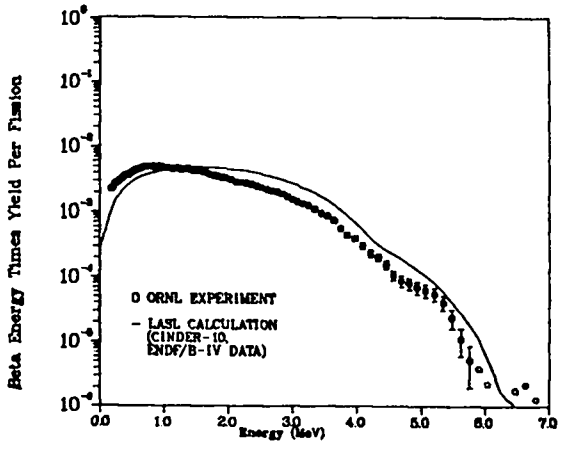

Fig. 19.
^{239}Pu thermal fission, 5 s irradiation, 5 s decay.

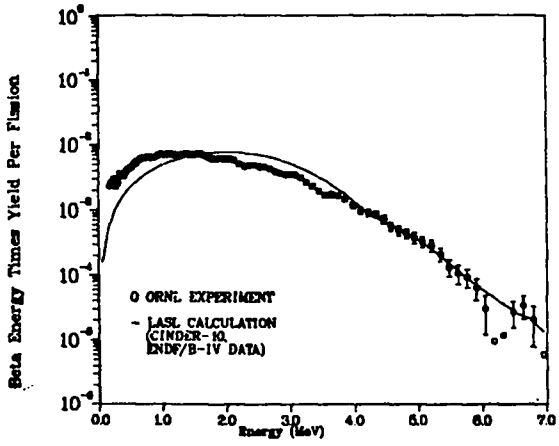

Fig. 20.
^{239}Pu thermal fission, 1 s irradiation, 29.7 s decay.

core curies for several nuclide groups. The groups are identified in Table VIII, and the curies are listed in Table IX.

D. Calculations in Support of LASL Non-Destructive Assay Methods (R. J. LaBauve, T. R. England, W. B. Wilson, and D. C. George)

LASL Group T-2 is currently providing support to LASL Group Q-5 (International Safeguards) in a program leading to the definition of measurable reactor spent-fuel properties accurately revealing fuel irradiation history and nuclide inventory. The T-2 calculations are to be performed with the current improved version of the EPRI-CINDER code[35] and library,[36] previously suppled to Q-5. It

TABLE VIII

DEFINITION OF ELEMENT GROUPS, TMI-2 TOTAL CORE CURIES

Element			Element Groups						
Name	Z	Sym	1	2	3	4	5	6	7
Selenium	34	Se						X	
Bromine	35	Br	X						
Krypton	36	Kr							X
Rubidium	37	Rb				X			
Strontium	38	Sr		X					
Yttrium	39	Y					X		
Zirconium	40	Zr					X		
Niobium	41	Nb					X		
Molybdenum	42	Mo			X				
Technetium	43	Tc			X				
Ruthenium	44	Ru			X				
Rhodium	45	Rh			X				
Palladium	46	Pd			X				
Antimony	51	Sb						X	
Tellurium	52	Te						X	
Iodine	53	I	X						
Xenon	54	Xe							X
Cesium	55	Cs				X			
Barium	56	Ba		X					
Lanthanum	57	La					X		
Cerium	58	Ce					X		
Praseodymium	59	Pr					X		
Neodymium	60	Nd					X		
Promethium	61	Pm					X		
Samarium	62	Sm					X		
Europium	63	Eu					X		
Neptunium	93	Np					X		
Plutonium	94	Pu					X		

is planned that the flux and shielded cross-section input needed for CINDER will be derived from the EPRI-CELL[37] code. EPRI-CELL also contains an old version of the EPRI-CINDER code, and final output from this module will be used for comparisons with our newer version of EPRI-CINDER. Complete comparisons cannot be made with EPRI-CELL alone because of the limited number of explicit nuclides in the EPRI-CELL library.

The initial T-2 effort centers on the demonstration of code-library validity in calculating nuclide inventories corresponding to measurements on spent-fuel samples from reactors specified by Q-5. The first set of measurements, the

TABLE IX

TOTAL CORE CURIES IN SELECTED TMI-2 NUCLIDE GROUPS[a]
(LASL CALCULATIONS 9/26/79)

Cooling Time	Group 1	Group 2	Group 3	Group 4	Group 5	Group 6	Group 7	Total Fission Products	Ac
1.0+0 s	1.11+9[b]	1.53+9	1.38+9	1.18+9	5.73+9	9.60+8	1.14+9	1.19+10	
4.0+0 s	1.05+9	1.43+9	1.37+9	1.05+9	5.36+9	9.20+8	1.06+9	1.11+10	
1.0+1 s	1.00+9	1.32+9	1.35+9	9.37+8	5.02+9	8.74+8	9.87+8	1.03+10	
4.0+1 s	8.49+8	1.10+9	1.27+9	7.76+8	4.42+9	7.70+8	8.23+8	8.80+9	
1.0+2 s	7.54+8	9.87+8	1.15+9	6.36+8	4.08+9	6.99+8	7.03+8	7.78+9	
4.0+2 s	6.63+8	8.31+8	9.09+8	4.24+8	3.72+9	5.83+8	5.34+8	6.40+9	
1.0+3 s	6.39+8	7.00+8	7.43+8	3.04+8	3.49+9	4.82+8	4.33+8	5.52+9	
1.0+0 h	5.77+8	5.13+8	5.06+8	1.37+8	3.15+9	2.91+8	3.44+8	4.25+9	
2.0+0 h	5.03+8	4.30+8	4.55+8	7.03+7	2.99+9	1.94+8	3.11+8	3.69+9	
5.0+0 h	3.87+8	3.21+8	4.30+8	2.55+7	2.71+9	1.34+8	2.68+8	3.06+9	
1.0+1 h	3.16+8	2.57+8	4.04+8	8.30+6	2.41+9	1.17+8	2.36+8	2.59+9	
2.0+1 h	2.42+8	2.14+8	3.67+8	2.01+6	2.03+9	1.02+8	2.00+8	2.14+9	
5.0+1 h	1.49+8	1.79+8	2.92+8	1.40+6	1.46+9	7.64+7	1.44+8	1.60+9	
1.0+2 h	9.27+7	1.62+8	2.13+8	1.35+6	1.02+9	4.99+7	1.08+8	1.26+9	
2.0+2 h	4.93+7	1.39+8	1.39+8	1.28+6	6.55+8	2.31+7	6.28+7	9.57+8	
5.0+2 h	1.21+7	9.03+7	8.73+7	1.13+6	4.02+8	5.19+6	1.24+7	6.07+8	
1.0+3 h	1.83+6	5.09+7	6.11+7	1.02+6	2.76+8	2.65+6	9.66+5	3.95+8	
2.0+3 h	4.99+4	2.37+7	3.18+7	9.65+5	1.72+8	1.27+6	1.07+5	2.30+8	
5.0+3 h	1.24+0	5.49+6	6.93+6	9.39+5	6.57+7	2.56+5	9.32+4	7.94+7	
1.0+0 y	1.92-1	2.05+6	3.11+6	9.16+5	2.93+7	1.03+5	9.06+4	3.55+7	
1.0+4 h	1.92-1	1.80+6	2.72+6	9.09+5	2.43+7	8.58+4	8.98+4	2.98+7	
2.0+4 h	1.92-1	1.52+6	1.21+6	8.59+5	9.06+6	4.03+4	8.34+4	1.26+7	
5.0+4 h	1.92-1	1.40+6	1.16+5	7.56+5	1.87+6	1.59+4	6.69+4	4.10+6	

[a] See Table VIII for listing of nuclides included in Groups 1-7.

[b] Read 1.11 + 9 as 1.11×10^9.

destructive analysis of samples from the H. B. Robinson-2 PWR plant,[38] is under investigation.

During this reporting period, effort centered on activating the EPRI-CELL code on the LASL LTSS operating system and linking the EPRI-CELL output to our improved version of EPRI-CINDER. The activiation of EPRI-CELL on LTSS is complete, and the linking with EPRI-CINDER is about 25% complete.

REFERENCES

1. D. C. Dodder and G. M. Hale, "Applications of Approximate Isospin Conservations in R-Matrix Analyses," in Neutron Physics and Nuclear Data (Proceedings, Harwell, 1978), p. 490 (1978).

2. G. M. Hale and D. C. Dodder, "Charge-Independent R-Matrix Analysis of the Four-Nucleon System," in Few Body Systems and Nuclear Forces II (Proceedings, Graz, 1978) p. 523 (1978).

3. T. W. Phillips, B. L. Berman, and J. D. Seagrave, "Neutron Total Cross Sections for Tritium," to be submitted to Phys. Rev. C (1979).

4. H. Rauch, "The Low Energy Neutron Scattering Lengths of the He^3 and T and Their Relation to the Four-Body Problem," in Few Body Systems and Nuclear Forces I (Proceedings, Graz, 1978), p. 289 (1978).

5. G. M. Hale and D. C. Dodder, "Scattering Lengths of n-^{3}He and n-T," in "Applied Nuclear Data Research and Development," Los Alamos Scientific Laboratory report LA-7843-PR, p. 2 (1979).

6. V. A. Sergeyev, "New ^{4}He Levels and the Difference in Angular Distributions for the Reactions D(d,n)^{3}He and D(d,p)^{3}H," Phys. Lett. 38B, 286 (1972).

7. J. P. Delaroche, Ch. Lagrange, and J. Salvy, "Nuclear Theory in Neutron Nuclear Data Evaluation," International Atomic Energy Agency report IAEA-190 (1976).

8. F. G. Perey, "Optical Model Analysis of Proton Elastic Scattering in the Range of 9 to 22 MeV," Phys. Rev. 131, 745 (1962).

9. Orlando F. Lemos, "Diffusion Elastique de Particules Alpha de 21 a 29.6 MeV sur des Noyaux de la Region Ti-Zn," Orsay report, series A136 (1972).

10. D. G. Gardner and M. A. Gardner, "Gamma-Ray Strength Functions in the Mass 90 Region," Bull. Am. Phys. Soc. 22, 993 (1977).

11. A. Gilbert and A. G. W. Cameron, "A Composite Nuclear-Level Density Formula with Shell Corrections," Can. J. Phys. 43, 1446 (1965).

12. J. L. Cook, H. Ferguson, and A. R. de L. Musgrove, "Nuclear Level Densities in Medium and Heavy Nuclei," Aust. J. Phys. 20, 477 (1967).

13. C. Kalbach, "The Griffin Model, Complex Particles and Direct Nuclear Reactions," Z. Phys. A283, 401 (1977).

14. G. S. Mani, "Spin Assignments to Excited States of ^{56}Fe Using Inelastic Proton Scattering," Nucl. Phys. A165, 225 (1971).

15. P. G. Young and E. D. Arthur, "GNASH: A Preequilibrium Statistical Model Code for Calculation of Cross Sections and Spectra," Los Alamos Scientific Laboratory report LA-6947 (1977).

16. R. Michel, G. Brinkmann, H. Weigel and W. Herr, "Measurements and Hybrid Analysis of Proton-Induced Reactions with V, Fe, and Co," Nucl. Phys. A322, 40 (1979).

17. I. L. Jenkins and A. G. Wain, "Excitation Functions for the Bombardment of ^{56}Fe with Protons," J. Inorg. Nucl. Chem. 32, 1419 (1970).

18. G. Clayeux and J. Voignier, "Diffusion Non Elastique de Neutrons de 14 MeV," C. E. de Lemeil report CEA-R-4279 (1972).

19. D. Hermsdorf, A. Meister, S. Sassonoff, D. Selliger, K. Seidel, and F. Shahin, "Differentielle Neutronenemissionsquerschitte bei 14.6 MeV Einschussenergie," Dresden report ZFK-277 (1974).

20. C. Kalbach, personal communication (1979).

21. B. E. Leshchenko, M. E. Gurtovoi, A. S. Kuklenko, and V. I. Strizhak, "Excitation of Collective States of Some Medium Nuclei by 14-MeV Neutrons," Sov. J. Nucl. Phys. 15, 5 (1972).

22. M. Hyakutake, M. Matoba, T. Tonai, J. Niidome, and S. Nakamura, "Scattering of 14.1 MeV Neutrons from Fe," J. Phys. Soc. Japan 38, 606 (1975).

23. G. T. Chapman, G. L. Morgan, and F. G. Perey, "A Re-Measurement of the Neutron-Induced Gamma-Ray Production Cross Sections for Iron in the Energy Range 850 keV $\leqslant E_n \leqslant$ 20.0 MeV," Oak Ridge National Laboratory report ORNL/TM-5416 (1976).

24. S. M. Grimes, R. C. Haight, K. R. Alvar, H. H. Barschall, and R. R. Borchers, "Charged-Particle Emission in Reactions of 15-MeV Neutrons with Isotopes of Chromium, Iron, Nickel, and Copper," Phys. Rev. C19, 2127 (1979).

25. T. Tamura, "Computer Program JUPITOR-1 for Coupled-Channel Calculations," Oak Ridge National Laboratory report ORNL-4152 (1967).

26. J. Raynal, Centre d'Etudes Nucleaires de Saclay, personal communication to D. Madland.

27. C. L. Dunford, "A Unified Model for Analysis of Compound Nucleus Reactions," Atomics International report AI-AEC-12931 (1970).

28. David G. Madland and J. Rayford Nix, "Calculation of Prompt Fission Neutron Spectra, Bull. Am. Phys. Soc. 24, 885 (1979).

29. H. Alter, R. B. Kidman, R. LaBauve, R. Protsik, and B. A. Zolatar, "ENDF-202 Cross Section Evaluation Working Group Benchmark Specifications," Brookhaven National Laboratory report BNL-19302 (1974).

30. P. D. Soran and R. J. Barrett, Los Alamos Scientific Laboratory, personal communication (1978).

31. R. B. Kidman and R. E. MacFarlane, "LIB-IV, A Library of Group Constants for Nuclear Reactor Calculations," Los Alamos Scientific Laboratory report LA-6260-MS (1976).

32. M. E. Battat, R. J. LaBauve, and D. W. Muir, "The GAMMON Activation Library," Los Alamos Scientific Laboratory report LA-8040-MS (1979).

33. T. R. England, R. E. Schenter, B. F. Rider, and J. R. Liaw, "Status of ENDF/B-V Yields," for presentation at the 3rd ASTM EURATOM Symposium on Reactor Dosimetry, Ispra, Italy (October 1-5, 1979).

34. T. R. England and W. B. Wilson, "TMI-2 Decay Power: LASL Fission-Product and Actinide Decay Power Calculations for the President's Commission on the Accident at Three Mile Island," Los Alamos Scientific Laboratory report LA-8041-MS (1979).

35. T. R. England, W. B. Wilson, and M. G. Stamatelatos, "Fission Product Data For Thermal Reactors, Part 2: Users Manual for EPRI-CINDER Code and Data," Electric Power Research Institute report EPRI NP-356, Part 2 (Dec. 1976). Also published as Los Alamos Scientific Laboratory report LA-6746-MS (Dec. 1976).

36. T. R. England, W. B. Wilson, and M. G. Stamatelatos, "Fission Product Data for Thermal Reactors, Part 1: A Data Set for EPRI-CINDER Using ENDF/B-IV," Electric Power Research Institute report EPRI NP/356, Part 1 (Dec. 1976). Also published as Los Alamos Scientific Laboratory report LA-6745-MS (Dec. 1976).

37. "ARMP: Advanced Recycle Methodology Program," Electric Power Research Institute report CCM-3 (Sept. 1977) (Proprietary), Chapter 5, Part II, "EPRI-CELL Code Description."

38. A. A. Bauer, L. M. Lowry, and J. S. Perrin, "Progress on Evaluating Strength and Ductility of Irradiated Zircaloy During July Through September, 1975," Battelle Columbus Laboratories report BMI-1938 (1975).

Printed in the United States of America. Available from
National Technical Information Service
US Department of Commerce
5285 Port Royal Road
Springfield, VA 22161

Microfiche $3.00

001-025	4.00	126-150	7.25	251-275	10.75	376-400	13.00	501-525	15.25
026-050	4.50	151-175	8.00	276-300	11.00	401-425	13.25	526-550	15.50
051-075	5.25	176-200	9.00	301-325	11.75	426-450	14.00	551-575	16.25
076-100	6.00	201-225	9.25	326-350	12.00	451-475	14.50	576-600	16.50
101-125	6.50	226-250	9.50	351-375	12.50	476-500	15.00	601-up	

Note: Add $2.50 for each additional 100-page increment from 601 pages up.